Supplementary Materials

Machine learning-assisted prediction, screen, and interpretation of porous carbon materials for high-performance supercapacitors

Hongwei Liu[1,2,3,#], Zhenming Cui[1,2,3,#], Zhennan Qiao[1,2,3], Xiaokang An[1,2,3], Yongzhen Wang[1,2,3,*]

[1]College of Materials Science and Engineering, Taiyuan University of Technology, Taiyuan 030024, Shanxi, China.
[2]Shanxi Joint Laboratory of Coal-based Solid Waste Resource Utilization and Green Development, Taiyuan University of Technology, Taiyuan 030024, Shanxi, China.
[3]Innovation Research Center for Materials Genetic Engineering, Taiyuan University of Technology, Taiyuan 030024, Shanxi, China.
[#]Authors contributed equally.

[*]**Correspondence to:** Prof. Yongzhen Wang, College of Materials Science and Engineering, Taiyuan University of Technology, 79 Yingze West Main Street, Taiyuan 030024, Shanxi, China. E-mail: wangyongzhen@tyut.edu.cn

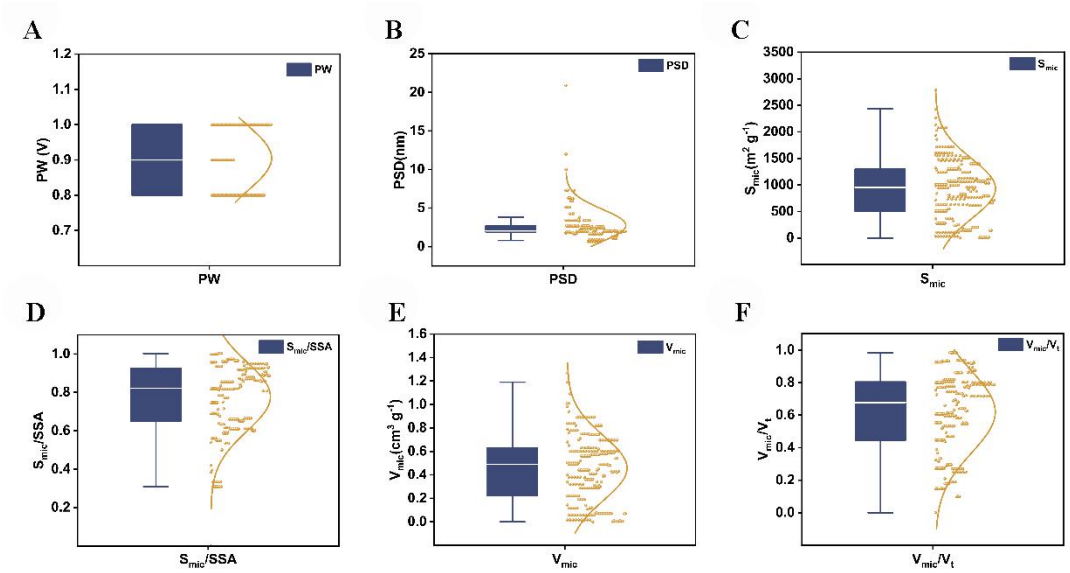

Supplementary Figure 1. Box-normal plots of the data distributions for each parameter of collected data. (A) Potential window (PW) tested in a three-electrode system, (B) Pore size distribution (PSD) of PCMs, (C) Micropore surface area (S_{mic}) of PCMs, (D) micropore surface area proportion (S_{mic}/SSA) of PCMs, (E) Micropore volume (V_{mic}), (F) Micropore volume proportion (V_{mic}/V_t).

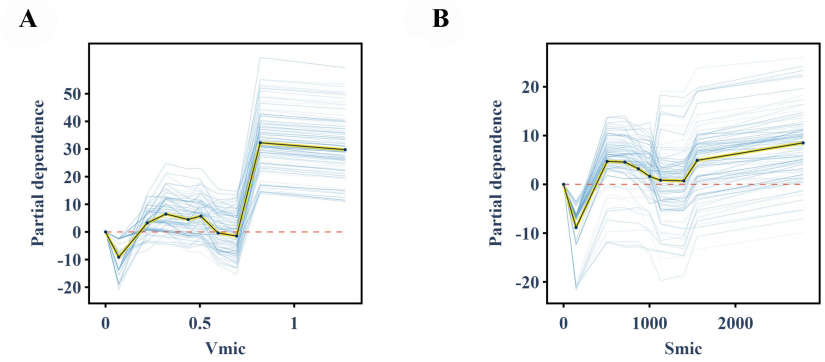

Supplementary Figure 2. One-dimensional partial dependence plots of (A) V_{mic} and (B) S_{mic}.

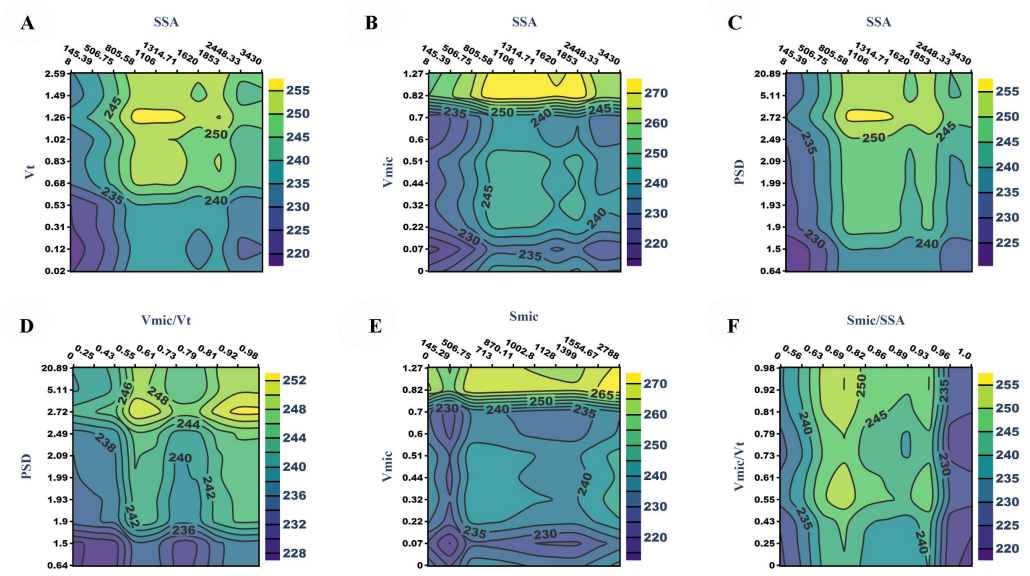

Supplementary Figure 3. Two-dimensional partial dependence plots of (A) SSA and V_t, (B) SSA and V_{mic}, (C) SSA and PSD, (D) V_{mic}/V_t and PSD, (E) S_{mic} and V_{mic}, and (F) S_{mic}/SSA and V_{mic}/V_t.

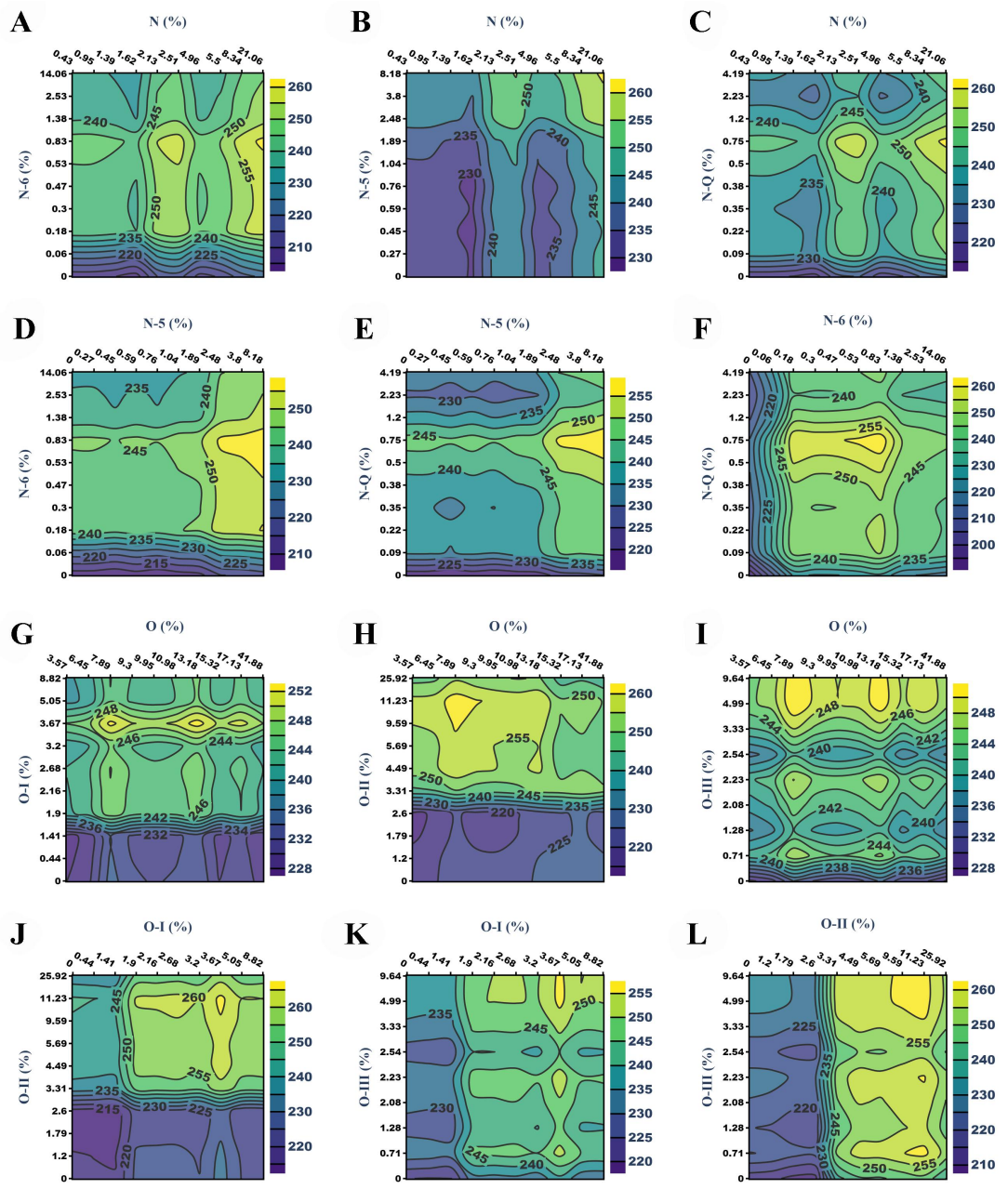

Supplementary Figure 4. Two-dimensional partial dependence plots of (A) N% and N-6%, (B) N% and N-5%, (C) N% and N-Q%, (D) N-5% and N-6%, (E) N-5% and N-Q%, (F) N-6% and N-Q%, (G) O% and O-I%, (H) O% and O-II%, (I) O% and O-III%, (J) O-I% and O-II%, (K) O-I% and O-III%, and (L) O-II% and O-III%.

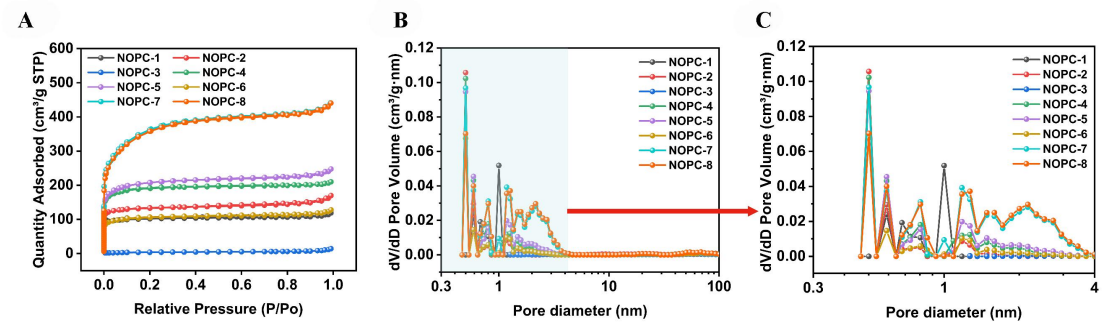

Supplementary Figure 5. (A) The N_2 adsorption desorption isotherms and (B) DFT pore-size distribution curves and (C) its local magnification of eight NOPC samples.

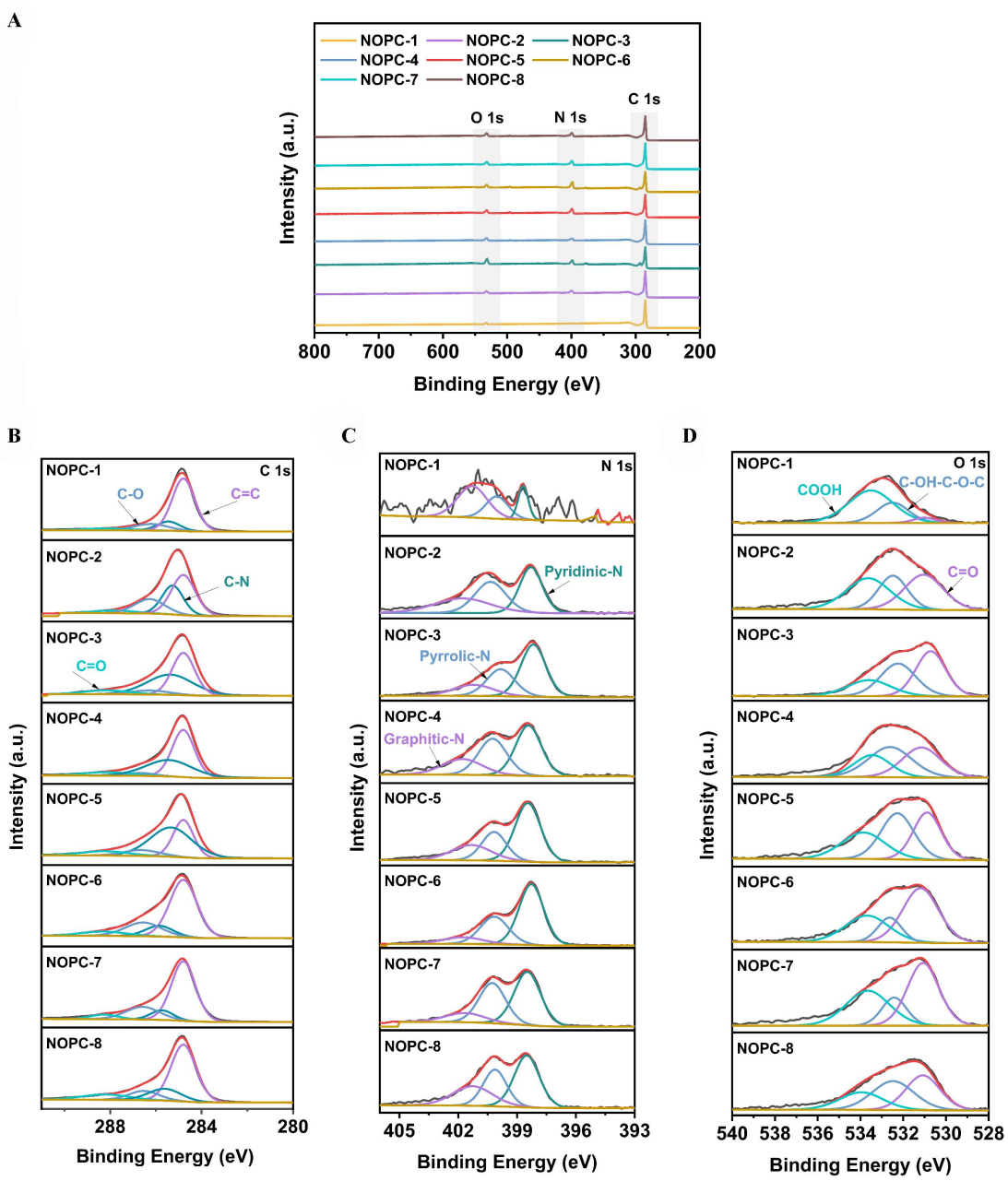

Supplementary Figure 6. (A) XPS survey spectra of eight NOPC samples, High resolution XPS spectra for (B) C 1 s, (C) N 1 s, and (D) O 1 s in eight NOPC samples.

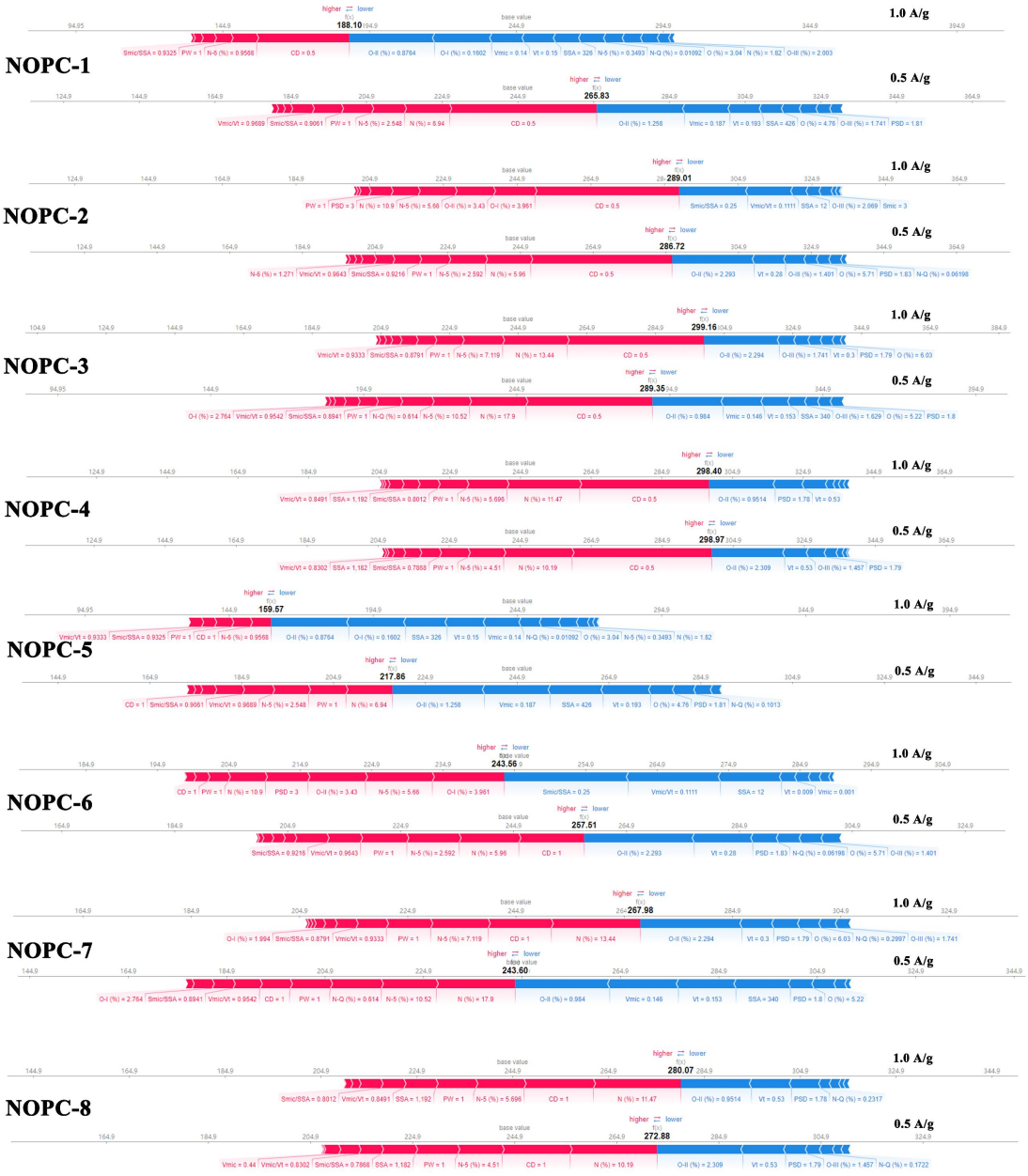

Supplementary Figure 7. Local SHAPs account for predictive biases in specific experimental NOPC samples from NOPC-1 to NOPC-8. Red represents positive influence, blue represents negative influence.

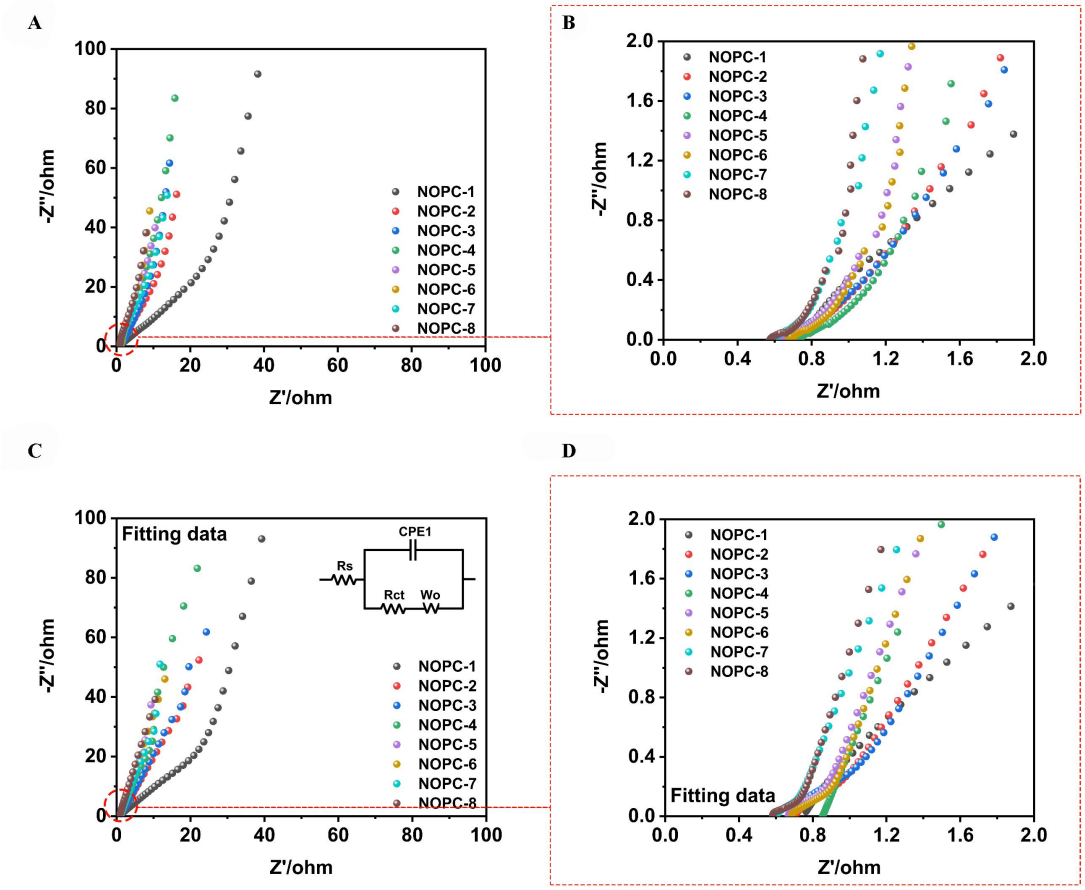

Supplementary Figure 8. (A) Nyquist plot of all NOPC samples, (B) the zoomed high-frequency region of all NOPC samples, (C) The fitted impedance curves of all NOPC samples, inset is the equivalent circuit diagram of impedance, (D) the zoomed high-frequency region of the fitted Nyquist plots of all NOPC samples.

Supplementary Table 1. Descriptive statistics of datasets

Data	Mean	Std.	Mean SE	Minimum	Median	Maximum	25%	50%	75%	Item
SC	241.32	76.60	4.62	5.44	245.46	547.00	200.00	245.46	288.03	Performance
CD	5.273	8.365	0.504	0.1	2	50	1	2	5	Test conditions
PW	0.9	0.09	0.006	0.8	0.9	1	0.8	0.9	1	
O	11.83	5.55	0.34	3.58	10.55	41.88	8.32	10.55	15.03	Element doping
N	4.00	4.01	0.24	0.43	2.45	21.06	1.41	2.45	5.16	
SSA	1286	880	53	8	1223	3430	615	1224	1745	Pore structure feature
V_t	0.83	0.61	0.04	0.02	0.79	2.59	0.36	0.79	1.16	
S_{mic}	930	562	34	0	954	2788	530	954	1296	
V_{mic}	0.46	0.27	0.02	0	0.49	1.27	0.26	0.49	0.63	
S_{mic}/SSA	0.78	0.18	0.01	0	0.82	1.00	0.65	0.82	0.92	
V_{mic}/V_t	0.62	0.25	0.02	0	0.68	0.98	0.44	0.68	0.80	
PSD	2.75	2.09	0.13	0.64	2.03	20.89	1.90	2.03	2.68	
N-6	1.22	2.28	0.14	0	0.49	14.06	0.20	0.49	1.01	Pseudocapacitive active site
N-5	1.55	1.48	0.09	0	0.91	8.18	0.46	0.91	2.24	
N-Q	0.81	0.84	0.05	0	0.47	4.19	0.22	0.47	1.18	

Data	Mean	Std.	Mean SE	Minimum	Median	Maximum	25%	50%	75%	Item
O-I	2.67	1.96	0.12	0	2.39	8.82	1.41	2.39	3.64	
O-II	5.43	5.04	0.30	0	3.98	25.92	2.30	3.98	8.00	Pseudocapacitive active site
O-III	2.33	1.96	0.12	0	2.15	9.64	0.91	2.15	2.95	

Supplementary Table 2. Pore structure parameters of eight NOPC samples

Samples	PSD [nm]	SSA [$m^2 g^{-1}$]	S_{mic} [$m^2 g^{-1}$]	S_{mic}/SSA	V_t [$cm^3 g^{-1}$]	V_{mic} [$cm^3 g^{-1}$]	V_{mic}/V_t
NOPC- 1	1.84	326	304	0.932	0.15	0.14	0.933
NOPC-2	1.81	426	386	0.906	0.193	0.187	0.969
NOPC-3	3.00	12	3	0.25	0.009	0.001	0.111
NOPC-4	1.83	612	564	0.921	0.28	0.27	0.964
NOPC-5	1.79	670	589	0.879	0.30	0.28	0.933
NOPC-6	1.80	340	304	0.894	0.153	0.146	0.954
NOPC-7	1.78	1192	955	0.801	0.53	0.45	0.849
NOPC-8	1.79	1182	930	0.787	0.53	0.44	0.83

Note: PSD, average pore diameter, PSD= 4 V_t/SSA; SSA, BET specific surface area; S_{mic}, micropore BET specific surface area; V_t, total pore volume; V_{mic}, micropore volume; S_{mic}/SSA, micropore surface area proportion; V_{mic}/V_t, micropore volume proportion.

Supplementary Table 3. Surface elemental content and N/O functional group content based on XPS results for the as-obtained eight NOPC samples

Samples	Surface elemental content based on XPS results			% of N1s for XPS			% of O1s for XPS		
	C	N	O	N-6	N-5	N-Q	C=O (O-I)	C-OH/C-O-C (O-II)	-COOH (O-III)
NOPC- 1	95.14	1.82	3.04	0.35	0.51	0.96	0.16	0.88	2.00
NOPC-2	88.3	6.94	4.76	2.55	2.38	2.01	1.76	1.26	1.74
NOPC-3	79.64	10.9	9.46	5.66	3.29	1.95	3.96	3.43	2.07
NOPC-4	88.33	5.96	5.71	2.59	2.10	1.27	2.02	2.29	1.4
NOPC-5	80.53	13.44	6.03	7.12	3.39	2.93	1.99	2.29	1.75
NOPC-6	76.88	17.9	5.22	10.52	5.49	1.89	2.76	0.83	1.63
NOPC-7	82.84	11.47	5.69	5.67	4.32	1.48	2.68	0.95	2.06
NOPC-8	83.78	10.19	6.03	4.51	2.98	2.7	2.26	2.31	1.46

Note: Pyridine nitrogen, N-6; Pyrrole nitrogen, N-5, Graphitic nitrogen, N-Q.

Supplementary Table 4. Charge transfer resistance and equivalent series resistance of the NOPC samples

Samples	Charge-transfer resistance (Rct) Ω	Equivalent series resistance (Res) Ω
NOPC-1	2.62	3.37
NOPC-2	0.42	1.12
NOPC-3	0.57	1.25
NOPC-4	0.36	1.21
NOPC-5	0.27	0.93
NOPC-6	0.04	0.72
NOPC-7	0.21	0.81
NOPC-8	0.003	0.58